

Lab Scale Experiments on Alumina Raft Formation

Sindre Engzelius Gylver, Asbjørn Solheim, Henrik Gudbrandsen, Åste Heggli Follo, and Kristian Etienne Einarsrud

Abstract During feeding of alumina into a Hall-Héroult cell, rafts floating on the bath surface may be formed. In this study, rafts were created in a laboratory furnace by adding 4 g secondary alumina in industrial bath. Samples were withdrawn from the bath in a time interval between 30 and 300 seconds. The experiments show that at 970°C, rafts will be formed within 30 seconds, and then slowly dissolve again with a constant rate of 0.8 g/min. Pores were found in the samples, giving extra buoyancy to the raft, thus increasing the floating time. Same experimental setup was used to investigate the effect of preheating of alumina, where it was found that coherent rafts will form up to at least 500°C.

Key words: Alumina Feeding, Rafts, Aluminum

Sindre Engzelius Gylver (corresponding author)
Department of Material Science and Engineering, NTNU
Tel.: +47 48252061
e-mail: sindre.e.gylver@ntnu.no

Asbjørn Solheim
SINTEF Industry
e-mail: Asbjorn.Solheim@sintef.no

Henrik Gudbrandsen
SINTEF Industry
e-mail: Henrik.Gudbrandsen@sintef.no

Åste Heggli Follo
Department of Material Science and Engineering, NTNU
e-mail: aste.heggli.follo@elkem.no

Kristian Etienne Einarsrud
Department of Material Science and Engineering, NTNU
Tel.: +47 97007236
e-mail: kristian.e.einarsrud@ntnu.no

1 Introduction

Alumina is the principal raw material used in the Hall-Héroult process in order to produce aluminum. As smelters reduce their bath volume and anode-cathode distance, efficient feeding and dissolution of alumina becomes more important. When alumina is added into the molten bath, it will have temperature below the liquidus of the bath. Temperature differences will lead to freezing of bath around the alumina particles, which will create floating agglomerates known as rafts. Formation of rafts is unfortunate, as it hinders dissolution of alumina, which might lead to anode effects. In addition, rafts may sink to the metal pad, or even further below, creating sludge. A better understanding of the mechanisms behind formation and dissolution of rafts is therefore crucial in order to obtain a more efficient feeding.

Formation of rafts in industrial cells has been observed in earlier work [1], where rafts were formed with floating times varying from 5 to 140 seconds. Anode age and thus available bath surface and circulation, as well as the acidity of the bath were suggested to have a significant effect on the floating time of the rafts. However, achieving detailed observations and recordings on industrial scale are difficult to accomplish due to the high temperature and hazardous gases.

Laboratory experiments give more controllable and reproducible conditions for raft formation. For instance, as demonstrated by Kaszás et al. [2], image analysis can be used to estimate thickness and surface area of rafts following alumina addition. See-through cells, where one can observe addition of alumina from the side is also a promising approach, and has been used to observe the behavior of alumina upon addition and the dissolution [3, 4]. X-ray furnaces have also been used for observations [5], demonstrating together with the other examples above that formations of rafts and agglomerates can be studied in detail.

Artificially produced agglomerates have been used as an alternative to alumina powder by several authors in order to achieve constant geometry and reproducible results. Walker et al. [5] packed alumina in a thin layer of aluminum foil, creating cylindrical shaped agglomerates. The agglomerates were immersed in bath and the mass gain as well as the thickness of the frozen layer as a function of time, temperature and AlF_3 concentration were measured. Increasing temperature and AlF_3 concentration yielded a smaller layer of frozen bath, which was explained with the increase of superheat, i.e the difference between the liquidus of the bath and temperature. The same setup has been adapted by several researches [6, 7], and also tested in industrial cells [8].

Use of cylindrical discs of compressed alumina is also a way of achieving a constant geometry, as demonstrated by Kaszás et al. [9]. Discs were removed after a certain floating time, and found that the density of the raft exceeded the bath's density, illustrating the effect surface tension will have on the floatability of rafts.

A comparison of agglomerates generated from both secondary and primary alumina shows that there will be more pores when secondary alumina is used [10]. The porosity was studied in the work by Yang et al. [4], whose samples contained porosities in 6-8 % range. The pores were explained by rapid release of hydroxyl and moisture upon additions into the bath. Computed Tomography (CT) on industrial

samples revealed that the distribution and size of pores will vary within a raft [11]. Pores will reduce the apparent density of rafts, thus contributing to buoyancy.

Pre-heating of alumina is a possibility to avoid raft formation. By adding hotter alumina, less bath will freeze around the particles, which may reduce raft formation. Hot exhaust gas has been investigated as a possible source of heat [12]. Experiments by Kobbeltvedt [6] suggest that preheating will result in more dispersed alumina, which will dissolve rapidly. For the alumina that will agglomerate, preheating had no positive effect, which was explained by decreased moisture content. Preheating will not assist the dissolution itself, which is suggested to be limited by mass transfer [13].

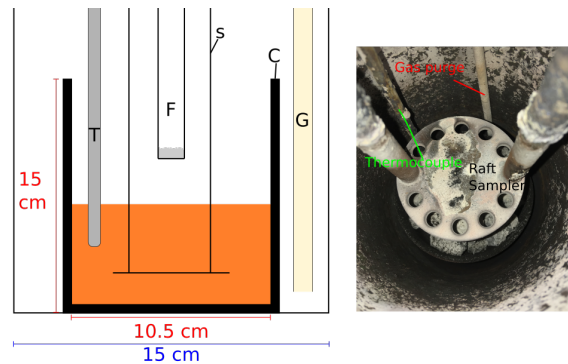
The current work investigates the behavior of alumina rafts, by adding alumina into an industrial bath, and removing agglomerates after a certain time. The goal is to create a setup that is closer to actually feeding in industrial cells, while still giving reproducible results. In such a setup, individual factors affecting dissolution can be studied in detail. In the present study, the effects of holding time as well as alumina temperatures on raft mass are investigated. Samples obtained from this setup were characterized with CT, which can be compared with samples of rafts from industrial cells [11].

2 Experimental details

2.1 Setup

The experiments were conducted in a custom-made open top furnace, consisting of a steel pipe with an inner diameter of 15 cm and a height of 41 cm. The furnace can be used for temperatures up to 1200°C, and it is heated by a heating element that winds around the pipe. During experiments, the top of the pipe was thermally insulated in order to preserve heat.

Fig. 1 Left: Vertical cross section of the furnace, equipped with thermocouple (T), feeding pipe (F), raft sampler (S), carbon crucible (C) and gas purge (G). Right: Image of the furnace seen from above.



A carbon crucible, with dimensions shown in figure 1, was filled with bath while nitrogen was purged into the furnace in order to avoid oxidation. Temperature was monitored with a S-type thermocouple placed inside a steel tube at the periphery of the crucible, immersed about 4 cm into the bath. A raft sampler was made in stainless steel, shaped as an 8 cm diameter plate with holes around its periphery. Feeding was done through a 50 cm long pipe with an inner diameter of 1 cm, equipped with a lid mounted on its bottom. The lid was actuated by a spring button on the top of the pipe. Alumina was released from about 5 cm above the bath surface. Alumina from two different suppliers were used in each of the two experiments described in sections 2.2 and 2.3. Although this in principle would introduce an additional uncertainty, the PSD and composition (determined by XRD, cf. tables 1 and 2) were so similar that the effect is believed to be negligible or at least comparable to other uncertainties in the setup

2.2 Formation and dissolution of rafts

Bath and alumina have properties described by table 1, where rafts were sampled at a bath temperature about 970 °C. The sampler with the created raft was withdrawn between 30 and 300 seconds after addition of alumina. After extraction of the ladle from the furnace, it was cooled in ambient conditions, before raft samples were removed and stored for further processing.

All samples were weighed and photographed after cooling and extraction from the ladle, and further post-processed in ImageJ [14] in order to calculate surface area.

Table 1 Physical data for the materials in the first set of experiments.

Bath Properties	Value
Bath acidity	10.8 wt%
Alumina content at start	2.3 wt %
Alumina Properties	Value
> 152.5 μm	9.7 %
44-152.5 μm	81.8 %
< 45 μm	8.5 %

2.3 Preheating

Properties of the bath and alumina are given in table 2, while the bath temperature was between 955 and 960 °C. 4 g alumina was added into the bath with a holding

time of 30 or 60 seconds, where a thermocouple was placed inside the feeding tube in order to monitor the temperature of the alumina. Removal and further image processing of rafts were performed as described in previous section (2.2).

Table 2 Physical data for the chemicals in the second set of experiments.

Bath Properties	Value
Bath acidity	10.9 wt%
Alumina content at start	2.1 wt %
Alumina Properties	Value
> 152.5 μm	8.7 %
44-152.5 μm	75.6 %
< 45 μm	15.7 %

2.4 Characterization

Selected rafts were cut and the cross sections were studied in a Nikon SMZ 800N optical Microscope. Micro computed X-ray tomography (μCT) was used to analyze the macroscopic structure. The data was acquired by a Nikon XT H225 ST instrument (cone beam volume CT), using a tungsten reflection target and an aluminum filter of 1 mm, with an acceleration voltage of 140 kV and a current of 220 μA . The imaging was done with an integration time of 1 s, amplification of 18 dB, with 3142 projections per 360°.

3 Results

The mass gain, i.e. the difference between the masses of formed raft and added alumina, as a function of holding time is shown in figure 2a), estimated to decrease with a rate of 0.8 g/min. A similar plot of surface area is given in figure 2b).

Surface area and variation of mass gain for different alumina temperatures are plotted in figure 3, where the holding time is 30 and 60 seconds for a) and b), respectively.

Images of selected non-preheated samples from optical microscopy and CT is shown in figure 4, while figure 5 shows calculated porosity and density of a raft. The porosity is reported as a percentage of pores relative to the entire horizontal cross-sectional area of the sample (including the pores), with an average porosity of 7.1 % for the samples analyzed.

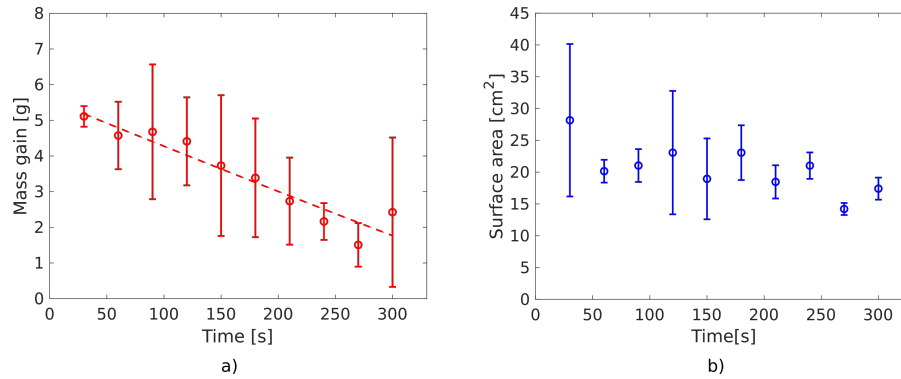


Fig. 2 a): Mean mass gain of rafts, given as the difference between raft weight and mass alumina added, and surface area (b) for holding times between 30 and 300 seconds and bath temperature of 970 °C. The error bars indicate a 95 % confidence interval. There are at least 3 measurements at each time.

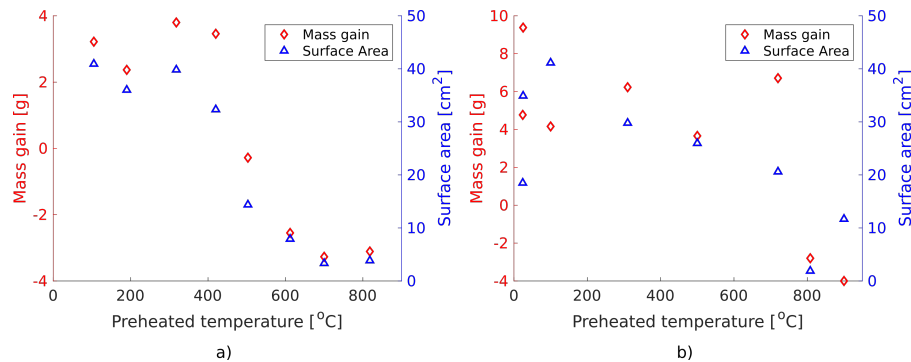


Fig. 3 Mass gain and surface area for different preheating temperatures. a) Holding time 30 seconds. b) Holding time 60 seconds. The bath temperature was between 955 and 960 °C.

4 Discussion and Conclusions

Alumina rafts have been created in a laboratory cell, where holding time and preheating of alumina were investigated.

As expected, bath freezes around cold alumina as it is added to the bath. Even at 970 °C, the mass gain is above the mass of alumina added to the bath. Melting of bath will then further reduce the mass of the rafts, as seen in figure 2a). At this temperature, the created rafts dissolve at 0.8 g/min, which is in the same order as found by Yang et al. [4].

The spread in data observed in 2 is believed to originate from two sources. Firstly, parts of the raft may have been lost during removal of the raft sampler from the furnace, thereby reducing the measured mass. Secondly, parts of the raft could remain on the sampler following extraction, again reducing the overall measured

Fig. 4 Images of the cross section of four different samples. a) Floating time 300 s, b) Floating time 90 s, c) floating time 60 s, d) floating time 210 s.

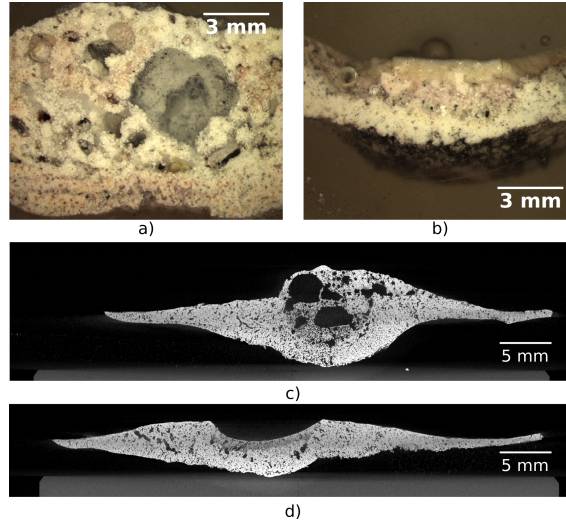
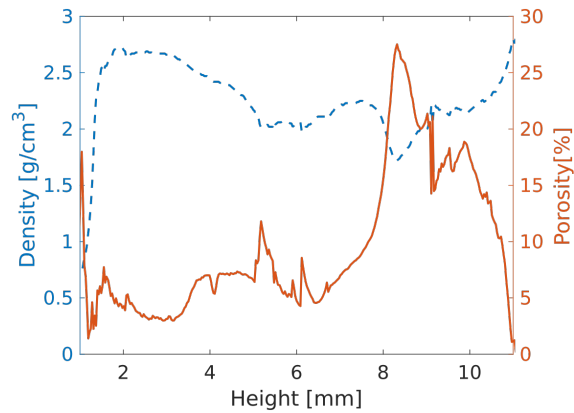
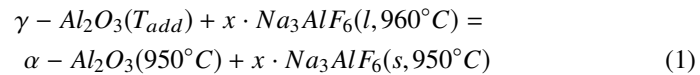


Fig. 5 Calculated density and porosity of sample with holding time 60 seconds and bath temperature 970 °C.



mass of the raft. As bath could freeze to the sampler independently of raft formation, it was not possible to quantify the mass loss of the raft by measuring the sampler weight before and after experiments.

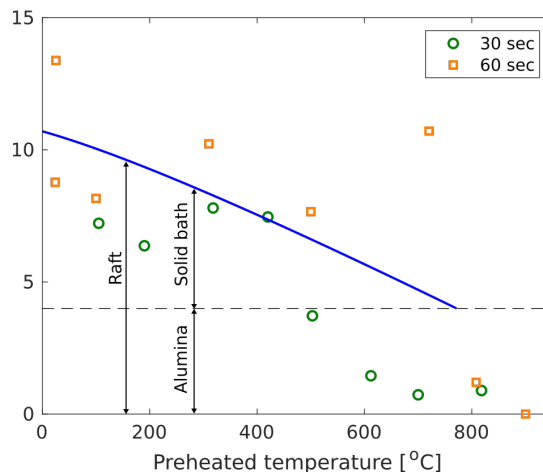
Figure 6 present calculated theoretical masses of rafts from the following reaction



where T_{add} is the temperature of added alumina, and x is the amount of cryolite required to freeze, represented by solid bath in the figure.

At low alumina temperatures, the calculated raft weight is lower than the theoretical one, which is probably because a fraction of the alumina batch will

Fig. 6 Theoretical mass of raft consisting of solid bath and alumina, assuming no initial dispersion and that all added alumina is converted from α to γ . Thermodynamical data from JANAF [15].



dissolve immediately [16]. At higher preheating temperatures, in particular for longer holding times, the weight is higher than the calculated effect. This could be due to infiltration of liquid bath inside of the raft, which will freeze upon sampling.

The effect of preheating (figure 3) shows that coherent rafts will form until alumina is heated to 500-600 °C. Above this temperature, most of the alumina will dissolve as dispersed particles. Since the dissolution of agglomerates is found to be controlled by mass transfer [13], preheating below 500 °C will have no effect on its dissolution time. The experiments by Kobbeltvedt [6] showed that more alumina will disperse at even lower temperatures. However, stirring was applied in his experiments, which will be beneficial for dispersion. In his experiments, the dissolution of agglomerates was rather unchanged with increased preheating temperature. Volatiles, in particular moisture, are found to have a positive effect on dissolution by breaking rafts apart [17]. Removal of these upon preheating will also create rafts that are harder to dissolve.

Preheating alumina up to 500-600 °C in an industrial cell might be challenging. Simulations indicate that this is possible by heat exchange of the exhaust gas [12], but measures must probably be taken to avoid that water vapor driven off in the hot zone condenses at the colder zones causing clogging. Preheating will require changes to traditional cell design and the effect on operational costs is uncertain.

Figure 4 illustrates the variation of the appearance of the rafts collected. While some will have large cavities covered around frozen bath (a) and c)), others contains a crater (b) and d)). Cavities are presented in earlier work [11] and believed to be formed due to moisture in alumina, which again lead to formation of water vapor and HF-gas. By assuming that alumina contains about 0.5 mass% moisture, 34 mL of water vapor will be released at 100°C and normal pressure [18]. This will be more than enough to create the pores and cavities observed. The craters could be formed in similar way, where the top of the layer has melted before collection. Pores and cavities will reduce the apparent density of the raft, hence increase its ability to float.

The trends found in apparent density and porosity (figure 5) are in the same range as those found in industrial rafts [11]. Laboratory rafts are much smaller, and some of them contain unproportionally large cavities. These cavities will contribute to very high calculated porosity. The real porosity of rafts should therefore be smaller in some areas.

The experimental setup gives possibilities to create alumina rafts under controlled conditions. In order to increase the relevance to industrial rafts, stirring should be considered. In addition, the mass of alumina added to available bath surface area is smaller in this setup than for an industrial cell, pointing out that dose size should be increased. Collection and further characterization of lab-induced rafts created under different conditions should increase the understanding of formation and dissolution rafts, thus pointing out ways for further technology development.

Acknowledgments The current work has been funded by SFI Metal Production (Centre for Research-based Innovation, 237738) and HighEFF (Centre for Environment-friendly Energy Research, 257632). The authors gratefully acknowledge the financial support from the Research Council of Norway and partners of the two centers.

References

1. S.E. Gylver, N.H. Omdahl, A.K. Prytz, A.J. Meyer, L.P. Lossius, K.E. Einarsrud, in *Light Metals 2019*, ed. by C. Chesonis (Springer International Publishing, 2019), pp. 659–666
2. C. Kaszás, L. Kiss, S. Poncsák, S. Guérard, J.F. Bilodeau, in *Light Metals 2017*, ed. by A.P. Ratvik (Springer, Cham, 2017), pp. 473–478
3. X. Liu, S.F. George, V.A. Wills, in *Light Metals 1994*, ed. by U. Mannweiler (1994), pp. 359–359
4. Y. Yang, B. Gao, Z. Wang, Z. Shi, X. Hu, *Journal of Metals* **67**(9), 2170 (2015)
5. D. Walker, T. Utigard, J. Toguri, M. Taylor, in *Advances in Production and Fabrication of Light Metals and Metal Matrix Composites*; (Edmonton, Alberta, Canada, 1992), pp. 23–37
6. O. Kobbeltvedt, Dissolution kinetics for alumina in cryolite melts : distribution of alumina in the electrolyte of industrial aluminium cells. Phd thesis, Norwegian University of Science and Technology, Department of Electrochemistry, Trondheim (1997)
7. N.P. Østbø, Evolution of alpha phase alumina in agglomerates upon addition to cryolitic melts. PhD Thesis, Norwegian University of Science and Technology - NTNU, Trondheim (2002)
8. D.I. Walker, T. Utigard, M.P. Taylor, in *Light Metals 1995*, ed. by J.W. Evans (TMS, 1995), pp. 425–434
9. C. Kaszás, L.I. Kiss, S. Poncsák, J.F. Bilodeau, S. Guérard, in *Proceedings of 34th International ICSOBA Conference* (Quebec, Canada, 2017)
10. S. Rolseth, J. Thonstad, in *Extraction, Refining, and Fabrication of Light Metals*, ed. by M. Sahoo, P. Pinfeld (Pergamon, Amsterdam, 1991), Proceedings of Metallurgical Society of Canadian Institute of Mining and Metallurgy, pp. 177–190
11. S.E. Gylver, N.H. Omdahl, S. Rørvik, I. Hansen, A. Nautnes, S.N. Neverdal, K.E. Einarsrud, in *Light Metals 2019*, ed. by C. Chesonis (Springer International Publishing, 2019), pp. 689–696
12. D.S. Severo, V. Gusberti, in *Proceedings of 35th International ICSOBA Conference*, vol. 46 (Hamburg, Germany, 2017), vol. 46, pp. 1059–1071
13. J. Thonstad, A. Solheim, S. Rolseth, O. Skar, in *Essential Readings in Light Metals: Volume 2 Aluminum Reduction Technology*, ed. by G. Bearne, M. Dupuis, G. Tarcy (Springer International Publishing, Cham, 2016), pp. 105–111
14. W. Rasband. ImageJ (1997). URL <https://imagej.nih.gov/ij/>

15. T. Allison. JANAF Thermochemical Tables, NIST Standard Reference Database 13 (1996). URL <http://kinetics.nist.gov/janaf/>
16. R.K. Jain, S. Tricklebank, B.J. Welch, D.J. Williams, in *Light Metals 1983*, ed. by E.M. Adkins (The Metallurgical Society of AIME, 1983), pp. 609–622
17. R.G. Haverkamp, Surface studies and dissolution studies of fluorinated alumina. PhD Thesis, The University of Auckland, Auckland (1992)
18. W. Wagner, *International Steam Tables : Properties of Water and Steam Based on the Industrial Formulation IAPWS-IF97*, 2nd edn. (Springer Berlin Heidelberg, 2008)